ACS chemical biology

Articles

pubs.acs.org/acschemicalbiology

Selective Detection of Caspase-3 versus Caspase-7 Using Activity-Based Probes with Key Unnatural Amino Acids

Chris J. Vickers, Gonzalo E. González-Páez, and Dennis W. Wolan*

Departments of Molecular and Experimental Medicine and Chemical Physiology, The Scripps Research Institute, La Jolla, California 92037, United States

Supporting Information

ABSTRACT: Caspases are required for essential biological functions, most notably apoptosis and pyroptosis, but also cytokine production, cell proliferation, and differentiation. One of the most well studied members of this cysteine protease family includes executioner caspase-3, which plays a central role in cell apoptosis and differentiation. Unfortunately, there exists a dearth of chemical tools to selectively monitor caspase-3 activity under complex cellular and *in vivo* conditions due to its close homology with executioner caspase-7. Commercially available activity-based probes and substrates rely on the canonical DEVD tetrapeptide sequence, which both caspases-3 and -7 recognize with similar affinity, and thus the individual contributions of caspase-3 and/or -7 toward important cellular processes are irresolvable. Here, we analyzed a variety of permutations of the DEVD peptide sequence in order to discover peptides with biased activity and recognition of caspase-3 versus caspases-6, -7, -8, and -9. Through this study, we identify fluorescent and biotinylated probes capable of selective detection of caspase-3 using key unnatural amino acids. Likewise, we determined the X-ray crystal structures of caspases-3, -7, and -8 in complex with our lead peptide inhibitor to elucidate the binding mechanism and active site interactions that promote the selective recognition of caspase-3 over other highly homologous caspase family members.

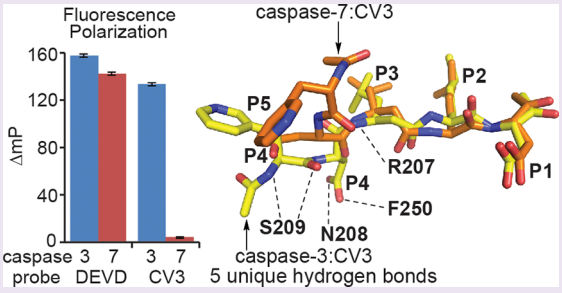

Caspases (cysteine-aspartyl proteases) are a family of enzymes predominantly linked with the initiation and execution of apoptosis,[1,2] as well as inflammation,[3,4] differentiation,[5−7] and cell survival.[8,9] Due to their consequential functions, caspases are typically stored as inactive proenzymes and are processed into the active form only when required.[10,11] Caspases most associated with apoptosis include the executioner caspases-3, -6, and -7 and the initiator caspases-8 and -9. Conversion of these enzymes from the zymogen into the active form occurs *in vivo* through processing by upstream proteases or self-activation that removes the N-terminal prodomain with subsequent cleavage of the protein into large and small subunits.[12,13] This internal cleavage allows for rearrangement of two large (17 kDa) and two small (12 kDa) subunits into a heterotetramer that composes the mature active enzyme.[14,15]

Activity-based probes (ABPs) have emerged as convenient and accessible tools to study protease function *in vitro* as well as in cellular and animal models. These probes measure and detect protease activity and can be applied toward elucidating the roles of proteases in the progression of diseases such as cancer,[16−21] neurodegenerative disorders,[22−25] and sepsis[26,27] or other biologically important phenomenon such as cell differentiation during development.[28] Additional techniques for studying enzyme activity that use ABPs include immunoprecipitation (IP), fluorescence microscopy, flow cytometry, fluorescent SDS-PAGE, fluorescence spectroscopy, and mass spectrometry-based proteomics.

ABPs employed in the detection of caspase activity typically contain a tag/label group for visualization (i.e., fluorophores) and/or enrichment (i.e., biotin), a peptide recognition sequence, and a thiol-reactive functional group for covalent modification of the active site catalytic cysteine. Cysteine-reactive functional groups commonly used to modify caspases include aldehydes, acyloxymethyl ketones (AOMKs), halomethyl ketones, epoxides, and Michael acceptors. Caspase ABPs typically contain a four-residue peptide recognition sequence (caspases-3/7: DEVD; caspase-6: VEHD; caspase-8: LETD; caspase-9: LEHD) established historically via combinatorial library optimization[29] and recently using unbiased mass spectrometry proteomic analyses.[30−32] This work laid the foundation for caspase-specific ABPs, substrates, and inhibitors; however, these peptide sequences lack functional selectivity within the caspase family, making recognition of a single caspase of interest extremely difficult.[33] ABPs, inhibitors, and substrates that are based on the DEVD peptide sequence recognize both caspases-3 and -7, thereby prohibiting study of the individual contribution of these enzymes toward biologically important events. Furthermore, DEVD-based probes also target caspases-6 and -8, further confounding the ability of the probe to exclusively target caspase-3.

Received: March 27, 2013
Accepted: April 24, 2013
Published: April 24, 2013

Customarily, new peptide sequences that recognize particular proteases are deduced through methods such as creation of positional-scanning combinatorial libraries (PSCL), which are useful starting points toward finding peptide sequences that recognize new enzyme targets.[34] Unfortunately, this method has limitations in providing information on optimized peptide sequences that are selective for one of two enzymes as closely related as active caspases-3 and -7 with 54% overall sequence identity and 77% active site identity (see Supplementary Table S1). Synergistic sequences or combinations of residues required for enhanced activity/selectivity are not easily recognized, and thorough analysis of every compound made in PSCLs is not feasible because residues are optimized only one at a time by combining the activity of thousands of other peptide sequences (for a tetrapeptide) into a single assay.[35] In addition to this drawback, the vast majority of research toward new peptide ABPs relies on natural amino acids that narrow the possibility of finding compounds with novel properties.[36,37] Therefore, we synthesized and analyzed a unique set of ABPs made from a pool of unnatural and natural amino acids that result in ABPs and inhibitors with selectivity for caspase-3 over caspase-7 and similar initiator and executioner caspases.

RESULTS AND DISCUSSION

Identification of Selective Caspase-3 Peptide Inhibitors. In order to find ABPs with selectivity for caspase-3 over caspase-7, we synthesized a library of inhibitors based on the DEVD peptide sequence. This tetrapeptide is labeled P4 (N-terminus) through P1 (C-terminus) and corresponds to the identity of the amino acids leading up to the invariable aspartic acid residue where caspases normally cleave their biologically relevant substrates.[38] We first selected a series of 30 amino acids, which we incorporated individually into each position of the canonical DEVD sequence (Figure 1). All synthesized peptides included an N-terminal acetyl group and a C-terminal aldehyde thiol-reactive moiety to generate caspase inhibitors (Figure 1). This series was designed to include primarily unnatural amino acids and hydrophobic natural residues in order to diversify beyond the standard amino acid chemistry (Supplementary Figure S1). All efforts to replace the P1 aspartic acid residue with glutamic acid or asparagine resulted in the ablation of inhibition (data not shown). As such, we built each subsequent inhibitor using standard solid-phase peptide synthesis (SPPS) from a P1 aspartic acid attached to a solid-supported aldehyde resin (Figure 1). Each residue within DEVD was individually substituted with our 30 amino acid set, resulting in 90 compounds exploring variations at P2, P3, and P4 (Figure 1). We also expanded the peptide to explore the effect of an additional residue at the P5 position where the 30 amino acids from our series were appended to the canonical DEVD sequence (Figure 1). In total, 120 potential caspase inhibitors were made by SPPS and cleaved from solid support with subsequent removal of the solvent. On the basis of the assumption that each inhibitor synthesis resulted in an approximate 15% overall yield, DMSO was added to each compound to produce 1 mM stock solutions. Relative IC_{50} values for recombinant caspase-3 and caspase-7 were then determined, and the ratio of the IC_{50} for caspase-7 over the IC_{50} for caspase-3 was plotted for each compound to elucidate any potential selectivity among the peptide library for inhibition of one of these highly homologous caspases over the other (Figure 1).

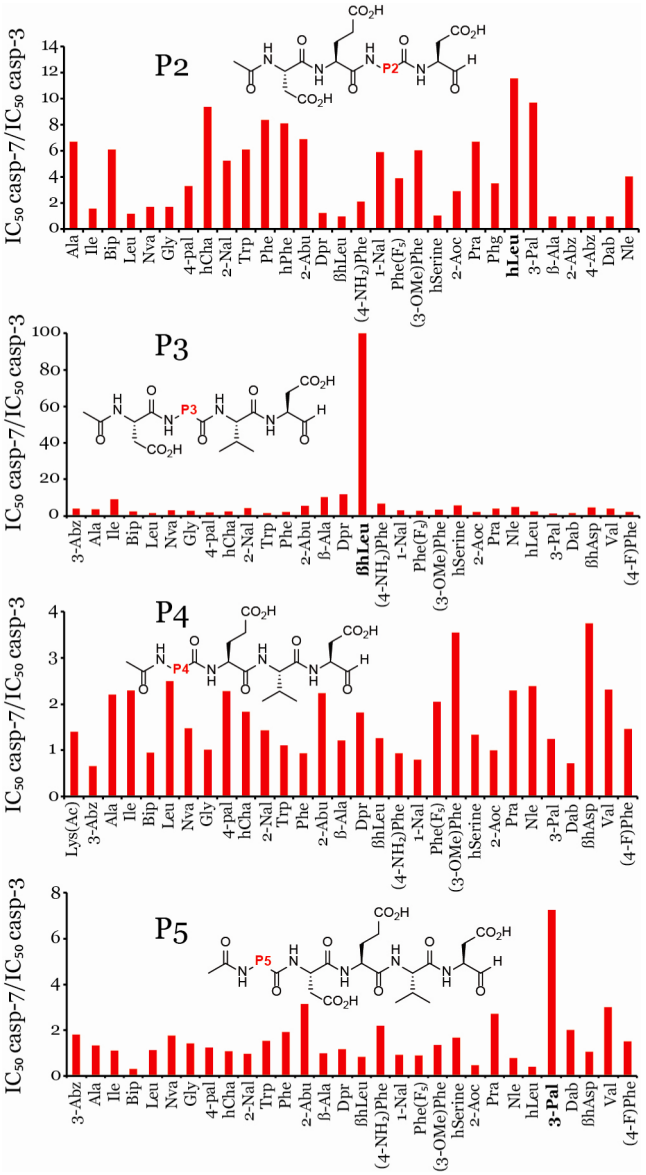

Figure 1. Caspase inhibitor selectivity screen using single amino acid substitutions at positions P2−P5. Residues that resulted in improved selectivity for caspase-3 used in subsequent probes are labeled bold.

In general, we found that substitutions from our amino acid pool into each position of the DEVD sequence imparted selectivity for caspase-3 inhibition (Figure 1). Replacement of glutamic acid at P3 with β-homoleucine provides the strongest contrast of inhibition for caspase-3 over caspase-7 with a 100-fold difference in relative IC_{50} values (Figure 1). Substitutions at P2 provide several compounds with an approximate 10-fold lower IC_{50} value for caspase-3 versus caspase-7, including unnatural amino acids homoleucine, 3-pyridylalanine, and homocyclohexylalanine (Figure 1). Less selectivity is obtained with amino acid variations at P4 compared to P2 or P3, and only two such substitutions, 3-methoxyphenylalanine and β-homoaspartic acid, have selectivity above 3-fold for inhibition of caspase-3 over caspase-7 (Figure 1). Appending a fifth amino acid to DEVD results in one example using 3-pyridylalanine with over 7-fold selectivity toward caspase-3 inhibition (Figure 1). Notably, no substitutions tested provided greater than 3-

dx.doi.org/10.1021/cb400209w | ACS Chem. Biol. 2013, 8, 1558−1566

Table 1. IC_{50} Values for Purified Caspase Inhibitors[a]

		IC_{50} (μM)				
	inhibitor	caspase-3	caspase-6	caspase-7	caspase-8	caspase-9
1	Ac-DEVD-CHO	0.021	0.048	0.040	0.038	2.0
2	Ac-D-βhLeu-hLeu-D-CHO	1.1	>200	66	>100	>100
3	Ac-(3-OMe)Phe-βhLeu-V-D-CHO	17	>200	86	>100	>100
4	Ac-D-βhLeu-3Pal-D-CHO	2.7	>200	24	>100	>100
5	Ac-βhAsp-βhLeu-hLeu-D-CHO	6.8	>100	110	29	>100
6	Ac-D-I-hLeu-D-CHO	0.39	>100	1.5	1.3	23
7	Ac-βhLeu-V-D-CHO	25	>200	19	27	>50
8	Ac-D-βhLeu-V-D-CHO	0.51	>100	17	6.8	>100
9	Ac-D-βhLeu-hLeu-D-AOMK	0.080	4.2	0.81	1.1	10
10	Ac-βhLeu-hLeu-D-AOMK	0.22	32	0.88	4.6	5.5
11	Ac-3Pal-D-βhLeu-hLeu-D-AOMK	0.023	3.4	0.73	0.40	4.6

[a]IC_{50} values represent averages of at least three separate experiments.

fold selectivity for inhibition of caspase-7 over caspase-3 (Figure 1).

We resynthesized several of the promising single amino acid substituted inhibitors in larger scale with subsequent prep-HPLC purification to validate our observed caspase-3 versus caspase-7 selectivity and to more accurately determine the IC_{50} values against executioner and initiator caspases (Table 1). For comparison to the canonical DEVD peptide recognition sequence, we also synthesized and determined IC_{50} values for Ac-DEVD-CHO (**1**) against caspases-3, -6, -7, -8, and -9 (Table 1). Inhibitor **1** has very similar IC_{50} values for caspases-3, -6, -7, and -8 as evidenced by the minimal 2-fold difference among these proteases (Table 1). We next synthesized **2** with homoleucine at P2 and β-homoleucine at P3, and this double substitution has a 60-fold lower IC_{50} for caspase-3 in comparison to caspase-7, with negligible inhibition of caspases-6, -8, and -9 (Table 1). Inhibitors combining β-homoleucine at P3 and either 3-methoxyphenylalanine (**3**) or β-homoaspartic acid (**5**) substitution at P4 result in significant loss in potency and selectivity toward caspase-3 (Table 1).

Compounds with β-homoleucine at P3 and 3-pyridylalanine (**4**) or valine (**8**) at P2 retain similar potency toward caspase-3 but drop in selectivity against caspase-7 (Table 1). Replacement of β-homoleucine at P3 with isoleucine (**6**) is undesirable as a complete loss in selectivity is observed, and removal of the P4 aspartic acid (**7**) results in a significant loss of efficacy toward caspase-3 and a reversal in selectivity toward greater inhibition of caspase-7 (Table 1).

We sought to translate our peptides from the reversible covalent aldehyde warhead into an irreversible AOMK derivative, which is useful for application of SDS-PAGE analysis and other labeling experiments. The AOMK contains an α-keto ester and binds the cysteine side chain irreversibly through loss of 2,6-dimethylbenzoic acid in an S_N2-like reaction. This type of warhead is commonly used in ABPs for caspases and has been shown to be more selective for caspase inhibition than other irreversible covalent modifying functional groups.[33] We replaced the C-terminal aldehyde of **2** with the keto ester to yield compound **9** (Table 1). Compared to **2**, **9** has greater than 10-fold more potency toward caspase-3 inhibition; however, selectivity versus caspase-7 dropped to only 10-fold (Table 1). Efforts to increase selectivity via removal of the P4 aspartic acid (**10**) resulted in less selectivity and was not pursued further (Table 1).

To enhance selectivity, we added 3-pyridylalanine as an extra residue at P5, which showed promising caspase-3 bias in our initial inhibitor screen (Figure 1). The resulting peptide (**11**) has an increase in potency toward inhibition of caspase-3 (23 nM) in comparison to **9** and a 32-fold selectivity over the caspase-7 IC_{50} (Table 1, Figure 2A). Importantly, **11** also has 150-fold selectivity for inhibition of caspase-3 over caspase-6, 17-fold selectivity versus caspase-8, and 200-fold selectivity over caspase-9 (Table 1). Further optimization of caspase-3 selective inhibitors could benefit by fixing P3 as β-homoleucine, which might favorably alter the specificity profiles of subsequent amino acid substitutions toward further selectivity for caspase-3 (Figure 1).

X-ray Structures of Inhibitor 11 in Complex with Caspases-3, -7, and, -8. In order to further investigate the mechanism of binding and specific interactions that promote selectivity for caspase-3, we determined the X-ray crystal structures of caspases-3, -7, and -8 in complex with **11** to 1.48, 2.94, and 1.18 Å, respectively (Figure 2B–H, Supplementary Table S2). Superposition of caspase-3 in complex with Ac-DEVD-CMK (PDB ID: 2DKO)[39] to our caspase-3 structure bound with **11** illustrates conserved interactions between the two inhibitors. Primarily the P1 and P2 residues coordinated to the active site C163 and hydrophobic pocket, respectively, as well as the P4 aspartic acid side chain that provides both inhibitors with a potential hydrogen bond to the F250 main-chain amide (Figure 2B,C). As a result of the β-amino acid substitution in **11**, the P3 side chains for the two inhibitors project in opposite directions with the β-homoleucine (**11**) directed into a hydrophobic pocket formed from the P2 homoleucine of **11** and W206, F256, and Y204 of caspase-3. For Ac-DEVD-CMK, the P3 glutamic acid residue forms a salt bridge with R207, and this important interaction is lost in **11** (Figure 2B). However, addition of the 3-pyridylalanine at P5 results in two extra potential hydrogen bonds between the P5 (**11**) main chain and S209 compared to the DEVD tetrapeptide (Figure 2B–D). These additional interactions help mitigate the loss of the P3 glutamic acid:R207 salt bridge between DEVD and the caspase-3 active site. As such, our optimized 5-residue inhibitor **11** and probes (**13**, **15**) retain almost identical IC_{50} values in comparison to the DEVD inhibitors with conserved C-terminal warheads (**12** and **14**, respectively) (Tables 1 and 2).

Superposition of caspases-3, -7, and -8 in complex with **11** reveal some similarities in peptide interactions among the three caspases. P1, P2, and P3 side-chain orientations with similar potential hydrophilic and hydrophobic interactions are conserved among the caspase active sites (Figure 2C–H).

dx.doi.org/10.1021/cb400209w | ACS Chem. Biol. 2013, 8, 1558–1566

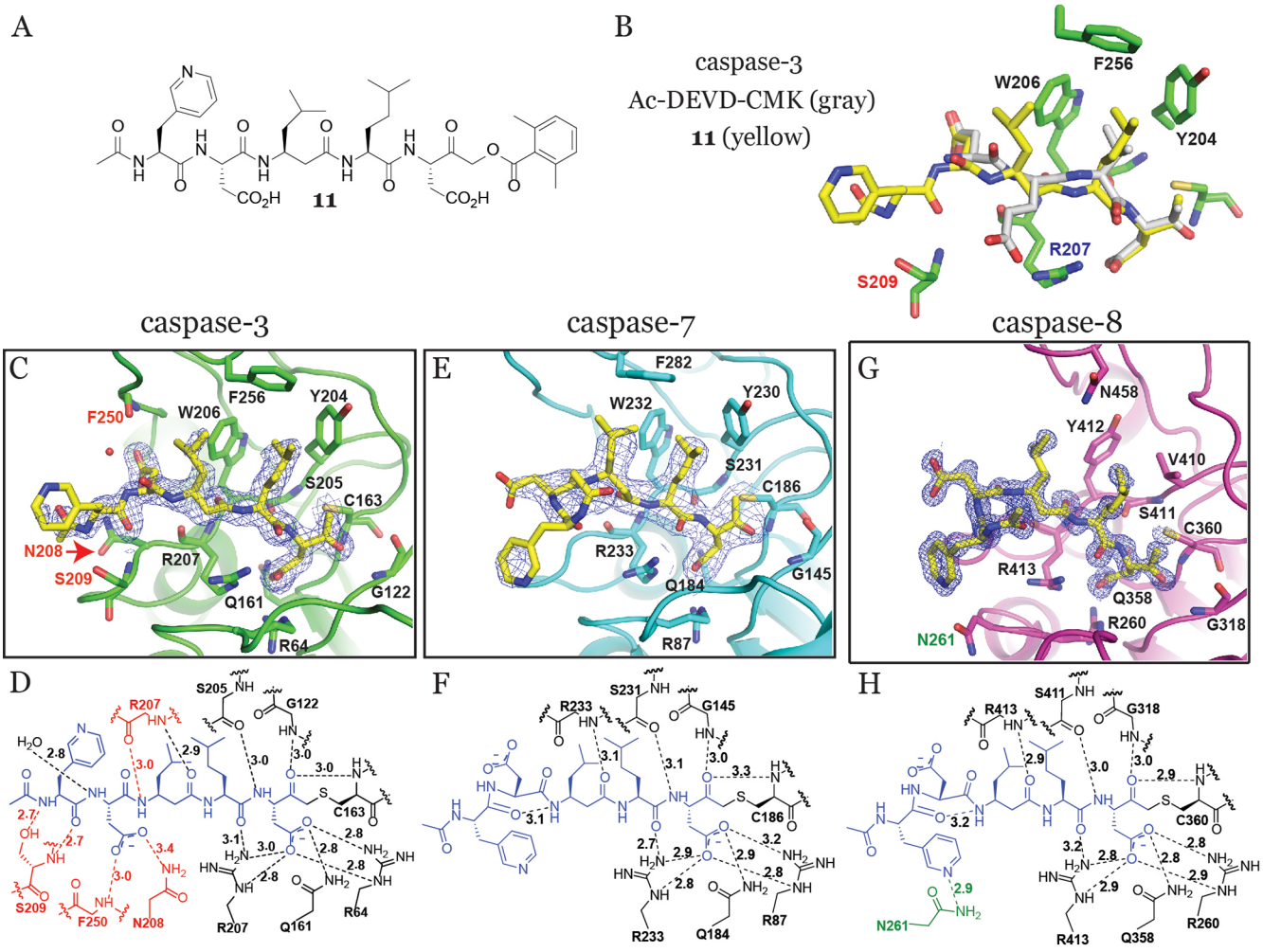

Figure 2. (A) Chemical structure of the caspase-3 specific peptide inhibitor **11** that contains three unnatural amino acids, an N-terminal acetyl, and a C-terminus AOMK warhead. (B) Residues of caspase-3 (carbon-green, oxygen-red, nitrogen-blue, and sulfur-dark yellow) bound to **11** (carbon-yellow) are shown as sticks. Superposition of Ac-DEVD-CMK from the co-complex with caspase-3 (PDB ID: 2DKO)[39] (carbon-gray) shows the additional hydrogen bonds provided by the P5 residue of **11** (red label) and loss of the salt bridge (blue label). (C) Cartoon representation of caspase-3 in complex with a stick representation of **11** (colors as in panel B). Specific main-chain and side-chain interactions provided by the caspase active site to the probe are labeled with an ordered water molecule depicted as a red sphere. A blue $2F_o - F_c$ electron density map contoured at 1.0σ show the ordered conformation of **11** within the active site of caspase-3. All unique potential hydrogen bonds provided by caspase-3 relative to caspases-7 and -8 are labeled red. (D) Schematic representation of the hydrogen bonding network and corresponding distances within the caspase-3 active site to **11** (blue). (E, F) Cartoon and schematic representations of caspase-7 (carbon-cyan) in complex with **11**, respectively, depict a rearrangement of the P4 and P5 residues of the probe resulting in a deficiency of potential hydrogen bonds to the caspase. All labels and colors are as in panels C and D. (G, H) Cartoon and schematic representations of caspase-8 (carbon-magenta) in complex with **11**, respectively. Similar to caspase-7, the P4 and P5 residues of **11** flip the P4 aspartic acid side chain into the solvent. One unique potential hydrogen bond is observed between the P5 pyridyl nitrogen of **11** and side-chain amide of N261 (labeled green in H). All labels and colors are as in panels C and D.

Table 2. IC_{50} Values for DEVD and CV3-Based Caspase ABPs[a]

		IC_{50} (nM)				
	inhibitor ID	caspase-3	caspase-6	caspase-7	caspase-8	caspase-9
12	FAM-DEVD-AOMK	18	26	24	29	1100
13	FAM-CV3-AOMK	27	3000	1300	100	3100
14	Biotin-DEVD-AOMK	39	75	38	50	1100
15	Biotin-CV3-AOMK	13	1200	420	53	2500

[a] IC_{50} values represent averages of at least three separate experiments.

However, the decreased hydrophobicity within the caspase-8 pocket, N458 compared to phenylalanine in caspase-3 (F256) and -7 (F282), may account for the decrease in ability to interact with the P2 homoleucine and P3 β-homoleucine of **11** (Figure 2C–H).

A crucial difference among the caspase structures is the conformation of the N-terminal residues of the peptide inhibitor. This region of **11** orients within the active sites of caspases-7 and -8 in a six-membered chair-like ring conformation with an intrapeptide hydrogen bond between the

dx.doi.org/10.1021/cb400209w | ACS Chem. Biol. 2013, 8, 1558–1566

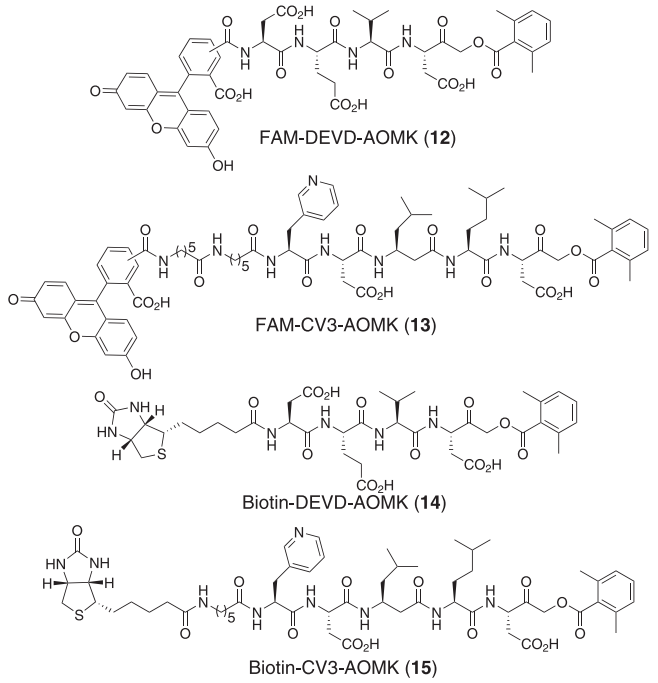

Figure 3. ABP structures using 5(6)-carboxyfluorescein (FAM) or biotin as a tag/label group. DEVD-based ABPs are routinely employed in caspase biology and are relatively nonselective for caspases-3, -6, -7, and -8. CV3 probes are based on our five-residue caspase-3-selective peptide recognition sequence of inhibitor **11**.

main-chain carbonyl oxygen of P5 (**11**) and the main-chain amide nitrogen of P4 (**11**) (Figure 2E−H). Surprisingly, **11** is locked into a linear and extended conformation in the caspase-3 active site, and this difference in orientation may provide the observed specific inhibition (Figure 2C,D). Due to the extended conformation within caspase-3, **11** can make additional hydrogen bonds between R207 and the P4 main-chain amide nitrogen (**11**), F250 and N208 to the P4 aspartic acid side chain (**11**), and S209 in two locations to the P5 main chain (**11**) (Figure 2C,D). The extended conformation of **11** within caspase-3 is due to 2 additional interactions provided by an active site S209, which is a proline in both caspases-7 (P235) and -8 (P415) (Figure 2C−H). As a consequence, the P5 pyridine and P4 aspartic acid side chains of **11** bound within caspases-7 and -8 rearrange into the chairlike ring conformation thereby flipping the aspartic acid away from the caspase active site and into the solvent (Figure 2E−H).

Strong electron density is observed for **11** in each co-complex except for the P5 pyridine side chain in the caspase-3 and -7 structures due to the lack of specific interactions to the caspase active sites. However, in caspase-8 the pyridine nitrogen of **11** shares a potential hydrogen bond with N261 resulting in strong electron density for the P5 pyridine side chain (Figure 2C, E, and G). Therefore, substitution of the pyridine nitrogen for a carbon in subsequent inhibitor design may impart additional selectivity for caspase-3 over caspase-8 (Figure 2G,H).

These structures illustrate the selectivity of **11** for caspase-3 as this co-complex has 15 potential hydrogen bonds between the inhibitor and the caspase-3 active site as well as strong hydrophobic interactions (Figure 2C,D). In contrast, caspases-7 (Figure 2E,F) and -8 (Figure 2G,H) have only 10 and 11 potential hydrogen bonds to **11**, respectively. The single substitution of P3 glutamic acid with β-homoleucine into the DEVD sequence (**8**) in our initial screen resulted in profound selectivity for caspases-3 over -7 (Figure 1). However, superposition of **11** bound to caspases-3 and -7 does not uncover significant differences in the P3 β-homoleucine orientation or active site interactions that can account for the observed assay specificity. We hypothesize that the extra methylene unit added within the peptide backbone upon β-homoleucine substitution (**8**) introduces additional hydrogen bonds between the carboxyl N-terminal acetyl group of **8** and S209 of caspase-3 as well as between the P3 amide nitrogen of **8** and R207 of caspase-3. We believe **8** adopts the intramolecular ring-like conformation similar to **11** when bound to caspase-7.

Synthesis and Application of Specific Caspase-3 ABPs. Our next goal was to apply our caspase-3 selective peptide inhibitors as ABPs by appending 5(6)-carboxyfluorescein (FAM) (**13**) or biotin (**15**) to the N-terminus of the optimized 5-residue sequence of **11** (Figure 3). Based on the X-ray structures, substitution of the N-terminal acetyl of **11** with FAM or biotin moieties would not affect the conformational selectivity of the peptide for caspase-3 as this region of the inhibitor is directed into the solvent when bound to all caspases (Figure 2C−H). We included a short linker region of 6-aminohexanoic acid (Ahx) for development of the ABPs that improves binding toward caspase-3 versus caspase-7 (Supplementary Figure S2).

The IC_{50} values for our CV3 series probes (ABPs that incorporate the unnatural amino acid sequence of inhibitor **11**) showed significant improvement compared to commonly used ABPs containing the canonical DEVD peptide recognition sequence as measured by kinetic substrate turnover assays (Table 2 and Figure 3). FAM-DEVD-AOMK (**12**) inhibits caspases-3, -6, -7, and -8 with almost identical IC_{50} values, whereas FAM-CV3-AOMK (**13**) inhibits caspase-3 with a 110-fold lower IC_{50} value than caspase-6, 48-fold lower than caspase-7, and 4-fold lower than caspase-8 (Table 2).

dx.doi.org/10.1021/cb400209w | *ACS Chem. Biol.* 2013, 8, 1558−1566

Consistently, Biotin-DEVD-AOMK (**14**) has similar IC_{50} values for caspases-3, -6, -7, and -8, while Biotin-CV3-AOMK (**15**) has a 92-fold lower IC_{50} value for caspase-3 versus caspase-6, 32-fold selectivity over caspase-7, and 4-fold selectivity compared to caspase-8 (Table 2). Interestingly, the fluorescein labeled probe (**13**) was more selective for caspase-3 over caspase-7 compared to the biotinylated probe (**15**), which may hint that additional residues beyond P5 may enhance caspase-3 specificity (Table 2). To further highlight the selectivity of our CV3 probes for caspase-3 over caspase-7, we compared the *in vitro* fluorescence polarization (FP) between FAM-DEVD-AOMK (**12**) or FAM-CV3-AOMK (**13**) (100 nM) and recombinant caspase-3 or caspase-7 (100 nM), which is within physiologically relevant concentrations (Figure 5).[40,41] Polarization of the fluorophore-tagged ABPs occur upon binding to the much larger caspase protein resulting in an increase in millipolarization (mP) that is directly read by a fluorescence plate reader (Figure 4).

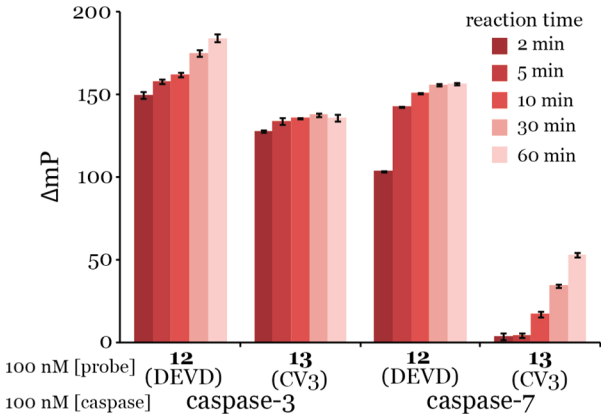

Figure 4. FP of binding **12** or **13** to caspase-3 or caspase-7 measured after 2, 5, 10, 30, or 60 min of incubation. Both probes and caspases were used at 100 nM final concentrations.

FAM-DEVD-AOMK (**12**) rapidly binds caspases-3 and -7, reaching nearly identical maximum ΔmP values within 2 min of introduction of the probe (Figure 4). In contrast, FAM-CV3-AOMK (**13**) rapidly reaches a maximum ΔmP values within 2 min only in the presence of caspase-3 (Figure 4). Reaction of FAM-CV3-AOMK (**13**) with caspase-7 occurs at a much slower rate with almost no detectable binding after 5 min of incubation and low levels of FP after an extended 60-min incubation (Figure 4). FAM-DEVD-AOMK (**12**) also shows robust FP when incubated with caspase-6, reaching ΔmP values >100 after only 5 min of incubation, whereas FAM-CV3-AOMK (**13**) shows almost no ΔmP after 10 min of incubation and less than 50 ΔmP after being allowed to react for 60 min (Supplementary Figure S3). FAM-CV3-AOMK (**13**) also shows slower association to caspase-8 compared to FAM-DEVD-AOMK (**12**); however, **13** peaks at a higher polarization intensity (Supplementary Figure S3).

To further explore the caspase-3 selectivity of FAM-CV3-AOMK (**13**) over FAM-DEVD-AOMK (**12**), we performed direct *in vitro* competition assays between recombinant caspase-3 and caspases-6, -7, or -8 (Figure 5). Equal concentrations (100 nM) of caspase-3 and either caspase-6, -7, or -8 were premixed followed by addition of varying concentrations of FAM-CV3-AOMK (**13**) or FAM-DEVD-AOMK (**12**) and subsequently incubated with the caspase mixture for 10 and 60 min. Samples were then analyzed by SDS-PAGE fluorescence to determine the extent of binding for each ABP to particular caspases (Figure 5). At stoichiometric concentrations of FAM-DEVD-AOMK (**12**) the probe binds almost exclusively to caspase-3 in the presence of caspase-6, -7, or -8 (Figure 5). However, at 4-fold to 16-fold excess probe, covalent attachment of the promiscuous FAM-DEVD-AOMK (**12**) occurs with caspases-6, -7, and -8 (Figure 5).

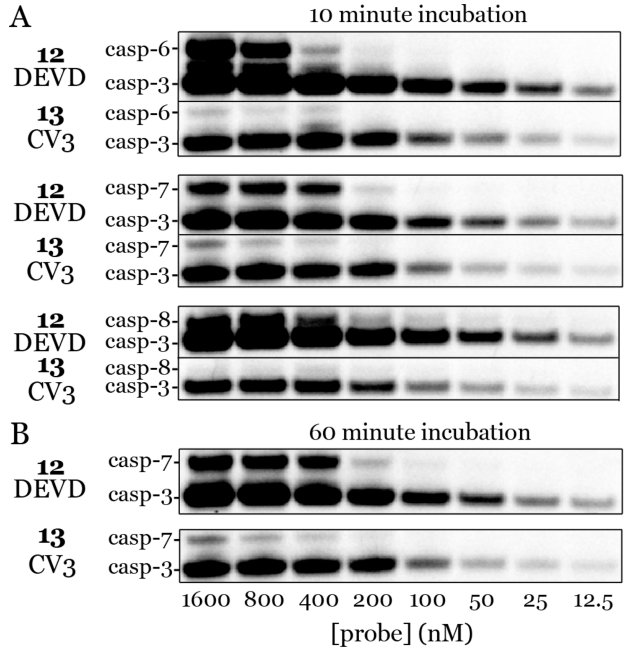

Figure 5. SDS-PAGE and fluorescent detection of varying concentrations of **12** or **13** incubated for either (A) 10 min or (B) 60 min with a premixed solution of caspase-3 and caspase-6, -7, or -8. Caspases were assayed at 100 nM final concentrations.

Conversely, FAM-CV3-AOMK (**13**) shows no significant covalent attachment to caspases-6, -7, or -8 even in the presence of 16-fold excess probe after 10 min of incubation (Figure 5A). In addition, after 60 min of incubation with 100 nM caspases-3 and -6, -7, or -8, FAM-CV3-AOMK (**13**) only significantly labels caspase-3 despite using 16-fold excess probe (Figure 5B and data not shown). Performing this same experiment with Biotin-DEVD-AOMK (**14**) and Biotin-CV3-AOMK (**15**) with SDS-PAGE followed by avidin blotting for biotin reveals a similar selectivity profile for Biotin-CV3-AOMK (**15**) caspase-3 selectivity, especially prevalent after 60 min of incubation between a premixture of caspase-3 and caspase-7 with the probes (Supplementary Figure S4).

In a follow-up competition experiment using 100 nM caspase-3 premixed with varying concentrations of either caspase-6, -7, or -8 (0 to 800 nM) followed by addition of 100 nM probe FAM-DEVD-AOMK (**12**) or FAM-CV3-AOMK (**13**), excess amounts of competing caspase-6, -7, or -8 could not bind to either probe in the presence of stoichiometric amounts of caspase-3 except at 8-fold excess compared to caspase-3 where trace amounts could be detected (Supplementary Figure S5). This result suggests that caspase-3 is kinetically faster than caspases-6, -7, or -8 in binding both ABPs (Supplementary Figure S5).

In order to confirm specificity of our ABP in a cell-based assay, we incubated HL-60 cells for 6 h with and without 1 μM

dx.doi.org/10.1021/cb400209w | *ACS Chem. Biol.* 2013, 8, 1558–1566

staurosporine (STS) to induce apoptosis and elicit the maturation of all apoptotic-related caspases (Figure 6). Cells

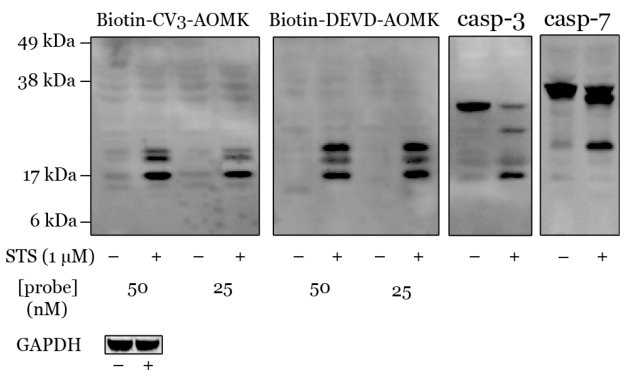

Figure 6. ABP labeling of HL-60 cells incubated for 6 h with or without 1 μM staurosporine. Cells were then lysed followed by addition of either 50 or 25 nM probe for 2 min. The right two panels are Western blots with caspase-3 or -7 antibody. Experiments were performed using the same cell lysate batch.

were lysed and incubated with Biotin-DEVD-AOMK (**14**) or Biotin-CV3-AOMK (**15**) at 50 or 25 nM for 2 min after which the reaction was quenched. Labeling was assessed by SDS-PAGE and avidin blotting to detect all proteins that were covalently modified by the ABPs within the cellular lysate (Figure 6). Biotin-DEVD-AOMK (**14**) labeled both caspases-3 and -7 almost identically at both 50 and 25 nM; however, lysate labeling with Biotin-CV3-AOMK (**15**) significantly decreased the amount of caspase-7 modification compared to the DEVD-based probe (Figure 6). Notably, no procaspase was labeled by either probe under the reaction conditions (Figure 6).

Caspases are essential for myriad biological processes from apoptosis to cell differentiation and inflammation. ABPs represent a convenient approach toward the study of these enzymes in a biological context; however, the lack of isoform-selective ABPs limits the ability to detect and probe the contribution of individual caspase enzymes within important biological phenomenon. To address this problem, we optimized a set of peptide-based caspase inhibitors using unnatural amino acids, which we successfully translated into functional ABPs. Increased structural diversity afforded by our unnatural amino acid pool enabled us to exploit small amino acid differences between the highly homologous caspase-3 and -7 active sites illustrating how adding structural diversity using unnatural amino acids can be helpful in future ABP development.

METHODS

Caspase Expression and Purification. Caspases-3, -6, -7, -8, and -9 were expressed and purified as previously described.[42,43]

Caspase-3 versus Caspase-7 Selectivity Screen. Compounds were synthesized using SPPS from an H-Asp(OtBu)-H preloaded aldehyde resin. Peptides were then cleaved from the resin followed by evaporation of the solvent. DMSO was used to make 1 mM stock solutions based on a 15% estimated overall yield. Compounds were then used without further purification.

IC_{50} Determination for Compounds against Recombinant Caspases. Compounds, caspases, and substrate were all diluted into assay buffer consisting of 50 mM HEPES pH 7.4, 0.1% CHAPS, 10 mM KCl, 50 mM sucrose, 1 mM $MgCl_2$, and 10 mM DTT. Twenty microliters of diluted compound (2.5×) and 20 μL of 2.5× caspase solution (final concentrations: 10 nM caspase-3, 50 nM caspase-6, 10 nM caspase-7, 25 nM caspase-8, or 500 nM caspase-9) was added to NUNC 96-well, black, low-binding, microtiter plates. This solution was incubated for 2 min at RT followed by addition of 10 μL (5×) caspase substrate at a final concentration of 50 μM (caspase-3/7: Ac-DEVD-AFC; caspase-6: Ac-VEID-AFC; caspase-8: Ac-IETD-AFC; or caspase-9: Ac-LEHD-AFC). The initial rate of substrate turnover (RFU/sec) was then immediately analyzed on a PerkinElmer EnVision plate reader with excitation at 355 nm and emission detection at 486 nm. This data was analyzed using GraphPad Prism to calculate corresponding IC_{50} values.

X-ray Crystallography of Caspases in Complex with Inhibitor. *Crystallization and X-ray Data Collection.* Inhibitor **11** was added in a 2-fold molar excess relative to 8 mg/mL caspases-3, -7, and -8 in a buffer consisting of 20 mM Tris, pH 8.0, 100 mM NaCl, incubated for 2 h at 25 °C and immediately used for co-crystallization experiments. Crystals of **11** in complex with caspase-3 were grown in 0.10 M sodium citrate, pH 6.5, 10 mM DTT, 0.1% sodium azide, 20% PEG 6000,[39] with caspase-7 in 0.15 M sodium citrate, pH 4.0, 2.0 M sodium formate,[44] and with caspase-8 in 0.1 M HEPES pH 7.4, 1.0 M sodium citrate.[45] All crystals were grown at 22 °C, and the His_6-tags were not removed as the proteins crystallized readily.

Data for all three caspase:**11** co-complex X-ray structures were collected on single, flash-cooled crystals at 100 K in a cryoprotectant consisting of mother liquor and 20% PEG 400 (caspase-3) or 25% glycerol (caspases-7 and -8) and were processed with HKL2000 in space groups $I222$ (caspase-3),[46] $P3_221$ (caspase-7), and $P3_121$ (caspase-8) (Supplementary Table S2). The asymmetric unit for caspases-3 and -8 contain one monomer of the biologically relevant homodimer and the complete homodimer for caspase-7. X-ray data for the caspase-3 and -8 complex:**11** structures were collected to 1.48 and 1.18 Å resolution, respectively, on beamline 11.1 at the Stanford Synchrotron Radiation Lightsource (SSRL) (Menlo Park, CA). For the caspase-7:**11** complex, data were collected to 2.94 Å resolution on the Advanced Photon Source (APS) beamline 23-ID-B at the Argonne National Laboratory (Argonne, IL). Data collection and processing statistics are summarized in Supplementary Table S2.

Structure Solution and Refinement. All caspase structures were determined by molecular replacement (MR) with Phaser[47,48] using the previously published caspase-3 (2DKO),[39] caspase-7 (1K86),[49] and caspase-8 (1QTN)[45] as the initial respective search models. All structures were manually built with Coot[50] and iteratively refined using Phenix[51] with cycles of conventional positional refinement. For the high-resolution caspase-3 and caspase-8 co-complex structures, anisotropic B-factor refinement was included. For the low-resolution caspase-7 structure, non-crystallographic symmetry restraints between the two subunits of the homodimer were applied during refinement. For all three structures, the electron density maps clearly identified that **11** was covalently attached to caspase active-site cysteine. Water molecules were automatically positioned by Phenix using a 2.5σ cutoff in $F_o - F_c$ maps and manually inspected. For the caspase-3 co-complex structure, the final R_{cryst} and R_{free} are 14.9% and 16.0%, respectively; for caspase-7, the final R_{cryst} and R_{free} are 18.9% and 21.6%, respectively; for caspase-8, the final R_{cryst} and R_{free} are 13.5% and 15.7% (Supplementary Table S2).

All models were analyzed and validated with PROCHECK,[48,52] WHATCHECK,[53] and Molprobity[54] on the Joint Center for Structural Genomics (JCSG) webserver. Analysis of backbone dihedral angles with the program PROCHECK[52] indicated that all residues for the three structures are located in the most favorable and additionally allowed regions in the Ramachandran plot. One aspartic acid residue of caspase-3 (D90) and -7 (D113) is positioned within the generously allowed region and contained in loop regions within both X-ray structures. Coordinates and structure factors have been deposited in the Protein Data Bank[55] with accession entries 4JJE (caspase-3), 4JJ8 (caspase-7), and 4JJ7 (caspase-8). Structure refinement statistics are shown in Supplementary Table S2.

Caspase Fluorescence Polarization (FP) Assay. Caspases and probes were diluted into assay buffer consisting of 50 mM HEPES pH 7.4, 0.1% CHAPS, 10 mM KCl, 50 mM sucrose, 1 mM $MgCl_2$, and 10 mM DTT. Twenty-five microliters of 2× recombinant caspase-3, -6, -7, or -8 (100 nM final concentration), followed by 25 μL of 2× FAM-DEVD-AOMK or FAM-CV3-AOMK (100 nM final concentration),

was added to NUNC 96-well, black, low-binding, microtiter plates. This solution was allowed to sit at RT for indicated time periods before the fluorescence polarization was read on a PerkinElmer EnVision plate reader with excitation at 480 nm and emission detection at 535 nm. ΔmP values are normalized by subtraction of control wells with probe only.

***In Vitro* ABP Caspase Selectivity Using SDS-PAGE.** Reducing SDS loading buffer was added to samples followed by boiling for 5 min and separation using SDS-PAGE. Fluorescein-labeled molecules were then imaged using a Hitachi FMBio II fluorescence flatbed scanner. Avidin blotting was used to visualize biotin-labeled samples.

Caspase Detection in Cell Lysates. HL-60 cells were cultured in RPMI media (10% FBS and Pen/Strep/Gln) at 37 °C with 5% CO_2. Cells were grown to a density of 500,000 cells/mL before addition of control media (DMSO 0.1%) or STS at a final concentration of 1 μM. Cells were then incubated at 37 °C for 6 h, centrifuged at 1000 rpm, and then lysed in assay buffer by Dounce homogenization. Lysates were then spun at 14,000 rpm for 30 min at 4 °C. The supernatant was taken, and aliquots were used for incubation with ABP (50 or 25 nM final concentration), Western blotting with caspase-3, -7 or GAPDH antibody, or addition of 0.1% DMSO. ABP and DMSO controls were avidin blotted for detection of labeled proteins.

■ ASSOCIATED CONTENT

Ⓢ Supporting Information

New compound characterization and X-ray crystallography data analysis. This material is available free of charge via the Internet at http://pubs.acs.org.

■ AUTHOR INFORMATION

Corresponding Author

*E-mail: wolan@scripps.edu.

Notes

The authors declare no competing financial interest.

■ ACKNOWLEDGMENTS

We thank I. Wilson, R. Stanfield, and M. Elsliger for helpful suggestions and computational assistance, B. Cravatt, H. Rosen, R. Ghadiri, and J. Paulson for instrumentation, the staff of SSRL beamline 11.1, and the staff of APS beamline 23-ID-B. We also gratefully acknowledge financial support from The Scripps Research Institute and the National Science Foundation (predoctoral fellowship to C.J.V.).

■ REFERENCES

(1) Riedl, J. R., and Shi, Y. (2004) Molecular mechanisms of caspase regulation during apoptosis. *Nat. Rev. Mol. Cell Biol. 5*, 897−907.

(2) Fuchs, Y., and Steller, H. (2011) Programmed cell death in animal development and disease. *Cell 147*, 742−758.

(3) Martin, S. J., Henry, C. M., and Cullen, S. P. (2012) A perspective on mammalian caspases as positive and negative regulators of inflammation. *Mol. Cell 46*, 387−397.

(4) Strowig, T., Henao-Mejia, J., Elinav, E., and Flavell, R. (2012) Inflammasomes in health and disease. *Nature 481*, 278−286.

(5) Fernando, P., Kelly, J. F., Balazsi, K., Slack, R. S., and Megeney, L. A. (2002) Caspase-3 activity is required for skeletal muscle differentiation. *Proc. Natl. Acad. Sci. U.S.A. 99*, 11025−11030.

(6) Fujita, J., Crane, A. M., Souza, M. K., Dejosez, M., Kyba, M., Flavell, R. A., Thomson, J. A., and Zwaka, T. P. (2008) Caspase activity mediates the differentiation of embryonic stem cells. *Cell Stem Cell 2*, 595−601.

(7) Larsen, B. D., Rampalli, S., Burns, L. E., Brunette, S., Dilworth, F. J., and Megeney, L. A. (2010) Caspase 3/caspase-activated DNase promote cell differentiation by inducing DNA strand breaks. *Proc. Natl. Acad. Sci. U.S.A. 107*, 4230−4235.

(8) Lamkanfi, M., Festjens, N., Declercq, W., Vanden Berghe, T., and Vandenabeele, P. (2007) Caspases in cell survival, proliferation and differentiation. *Cell Death Differ. 14*, 44−55.

(9) Kikuchi, M., Kuroki, S., Kayama, M., Sakaguchi, S., Lee, K. K., and Yonehara, S. (2012) Protease activity of procaspase-8 is essential for cell survival by inhibiting both apoptotic and nonapoptotic cell death dependent on receptor-interacting protein kinase 1 (RIP1) and RIP2. *J. Biol. Chem. 287*, 41165−41173.

(10) Boatright, K. M., and Salvesen, G. S. (2003) Mechanisms of caspase activation. *Curr. Opin. Cell Biol. 15*, 725−731.

(11) Pop, C., and Salvesen, G. S. (2009) Human caspases: activation, specificity, and regulation. *J. Biol. Chem. 284*, 21777−21781.

(12) Salvesen, G. S., and Dixit, V. M. (1999) Caspase activation: the induced-proximity model. *Proc. Natl. Acad. Sci. U.S.A. 96*, 10964−10967.

(13) Shi, Y. (2004) Caspase activation: revisiting the induced proximity model. *Cell 117*, 855−858.

(14) Feeney, B., and Clark, A. C. (2005) Reassembly of active caspase-3 is facilitated by the propeptide. *J. Biol. Chem. 280*, 39772−39785.

(15) Keller, N., Grütter, M. G., and Zerbe, O. (2010) Studies of the molecular mechanism of caspase-8 activation by solution NMR. *Cell Death Differ. 17*, 710−718.

(16) Joyce, J. A., Baruch, A., Chehade, K., Meyer-Morse, N., Giraudo, E., Tsai, F. Y., Greenbaum, D. C., Hager, J. H., Bogyo, M., and Hanahan, D. (2004) Cathepsin cysteine proteases are effectors of invasive tumor growth and angiogenesis during multistage tumorigenesis. *Cancer Cell 5*, 443−453.

(17) Speers, A. E., and Cravatt, B. F. (2004) Profiling enzyme activities *in vivo* using click chemistry methods. *Chem. Biol. 11*, 535−546.

(18) Paulick, M. G., and Bogyo, M. (2008) Application of activity-based probes to the study of enzymes involved in cancer progression. *Curr. Opin. Genet. Dev. 18*, 97−106.

(19) Edgington, L. E., Berger, A. B., Blum, G., Albrow, V. E., Paulick, M. G., Lineberry, N., and Bogyo, M. (2009) Noninvasive optical imaging of apoptosis by caspase-targeted activity-based probes. *Nat. Med. 15*, 967−973.

(20) Nomura, D. K., Dix, M. M., and Cravatt, B. F. (2010) Activity-based protein profiling for biochemical pathway discovery in cancer. *Nat. Rev. Cancer 10* (630), 638.

(21) Edgington, L. E., Verdoes, M., Ortega, A., Withana, N. P., Lee, J., Syed, S., Bachmann, M. H., Blum, G., and Bogyo, M. (2013) Functional imaging of legumain in cancer using a new quenched activity-based probe. *J. Am. Chem. Soc. 135*, 174−182.

(22) Graham, R. K., Deng, Y., Slow, E. J., Haigh, B., Bissada, N., Lu, G., Pearson, J., Shehadeh, J., Bertram, L., Murphy, Z., Warby, S. C., Doty, C. N., Roy, S., Wellington, C. L., Leavitt, B. R., Raymond, L. A., Nicholson, D. W., and Hayden, M. R. (2006) Cleavage at the caspase-6 site is required for neuronal dysfunction and degeneration due to mutant huntingtin. *Cell 125*, 1179−1191.

(23) Leyva, M. J., Degiacomo, F., Kaltenbach, L. S., Holcomb, J., Zhang, N., Gafni, J., Park, H., Lo, D. C., Salvesen, G. S., Ellerby, L. M., and Ellman, J. A. (2010) Identification and evaluation of small molecule pan-caspase inhibitors in Huntington's disease models. *Chem. Biol. 17*, 1189−1200.

(24) Edgington, L. E., van Raam, B. J., Verdoes, M., Wierschem, C., Salvesen, G. S., and Bogyo, M. (2012) An optimized activity-based probe for the study of caspase-6 activation. *Chem. Biol. 19*, 340−352.

(25) D'Amelio, M., Sheng, M., and Cecconi, F. (2012) Caspase-3 in the central nervous system: beyond apoptosis. *Trends Neurosci. 35*, 700−709.

(26) Hotchkiss, R. S., Chang, K. C., Swanson, P. E., Tinsley, K. W., Hui, J. J., Klender, P., Xanthoudakis, S., Roy, S., Black, C., Grimm, E., Aspiotis, R., Han, Y., Nicholson, D. W., and Karl, I. E. (2000) Caspase inhibitors improve survival in sepsis: a critical role of the lymphocyte. *Nat. Immunol. 1*, 496−501.

(27) Hotchkiss, R. S., and Nicholson, D. W. (2006) Apoptosis and caspases regulate death and inflammation in sepsis. *Nat. Rev. Immunol. 6*, 813−822.
(28) Kuranaga, E. (2011) Caspase signaling in animal development. *Dev. Growth Differ. 53*, 137−148.
(29) Thornberry, N. A., Rano, T. A., Peterson, E. P., Rasper, D. M., Timkey, T., Garcia-Calvo, M., Houtzager, V. M., Nordstrom, P. A., Roy, S., Vaillancourt, J. P., Chapman, K. T., and Nicholson, D. W. (1997) A combinatorial approach defines specificities of members of the caspase family and granzyme B. *J. Biol. Chem. 272*, 17907−17911.
(30) Mahrus, S., Trinidad, J. C., Barkan, D. T., Sali, A., Burlingame, A. L., and Wells, J. A. (2008) Global sequencing of proteolytic cleavage sites in apoptosis by specific labeling of protein N-termini. *Cell 134*, 866−876.
(31) Dix, M. M., Simon, G. M., and Cravatt, B. F. (2008) Global mapping of the topography and magnitude of proteolytic events in apoptosis. *Cell 134*, 679−691.
(32) O'Donoghue, A. J., Eroy-Reveles, A. A., Knudsen, G. M., Ingram, J., Zhou, M., Statnekov, J. B., Greninger, A. L., Hostetter, D. R., Qu, G., Maltby, D. A., Anderson, M. O., Derisi, J. L., McKerrow, J. H., Burlingame, A. L., and Craik, C. S. (2012) Global identification of peptidase specificity by multiplex substrate profiling. *Nat. Methods 9*, 1095−1100.
(33) Berger, A. B., Sexton, K. B., and Bogyo, M. (2006) Commonly used caspase inhibitors designed based on substrate specificity profiles lack selectivity. *Cell Res. 16*, 961−963.
(34) Choe, Y., Leonetti, F., Greenbaum, D. C., Lecaille, F., Bogyo, M., Brömme, D., Ellman, J. A., and Craik, C. S. (2006) Substrate profiling of cysteine proteases using a combinatorial peptide library identifies functionally unique specificities. *J. Biol. Chem. 281*, 12824−12832.
(35) Thornberry, N. A., Chapman, K. T., and Nicholson, D. W. (2000) *Methods Enzymol. 322*, 100−110.
(36) Dougherty, D. A. (2000) Unnatural amino acids as probes of protein structure and function. *Curr. Opin. Chem. Biol. 4*, 645−652.
(37) Berger, A. B., Witte, M. D., Denault, J. B., Sadaghiani, A. M., Sexton, K. M., Salvesen, G. S., and Bogyo, M. (2006) Identification of early intermediates of caspase activation using selective inhibitors and activity-based probes. *Mol. Cell 23*, 509−521.
(38) Shimbo, K., Hsu, G. W., Nguyen, H., Mahrus, S., Trinidad, J. C., Burlingame, A. L., and Wells, J. A. (2012) Quantitative profiling of caspase-cleaved substrates reveals different drug-induced and cell-type patterns in apoptosis. *Proc. Natl. Acad. Sci. U.S.A. 109*, 12432−12437.
(39) Ganesan, R., Mittl, P. R. E., Jelakovic, S., and Grütter, M. G. (2006) Extended substrate recognition in caspase-3 revealed by high resolution X-ray structure analysis. *J. Mol. Biol. 359*, 1378−1388.
(40) Pop, C., Chen, Y. R., Smith, B., Bose, K., Bobay, B., Tripathy, A., Franzen, S., and Clark, A. C. (2001) Removal of the pro-domain does not affect the conformation of the procaspase-3 dimer. *Biochemistry 40*, 14224−14235.
(41) Svingen, P. A., Loegering, D., Rodriquez, J., Meng, X. W., Mesner, P. W., Holbeck, S., Monks, A., Krajewski, S., Scudiero, D. A., Sausville, E. A., Reed, J. C., Lazebnik, Y. A., and Kaufmann, S. H. (2004) Components of the cell death machine and drug sensitivity of the National Cancer Institute Cell Line Panel. *Clin. Cancer Res. 10*, 6807−6820.
(42) Denault, J. B., and Salvesen, G. S. (2003) Expression, purification, and characterization of caspases. *Curr. Protoc. Protein Sci.* Chapter 21:Unit 21.13.
(43) Wolan, D. W., Zorn, J. A., Gray, D. C., and Wells, J. A. (2009) Small-molecule activators of a proenzyme. *Science 326*, 853−858.
(44) Feldman, T., Kabaleeswaran, V., Jang, S. B., Antczak, C., Djaballah, H., Wu, H., and Jiang, X. A (2012) Class of allosteric caspase inhibitors identified by high-throughput screening. *Mol. Cell 47*, 585−595.
(45) Watt, W., Koeplinger, K. A., Mildner, A. M., Heinrikson, R. L., Tomasselli, A. G., and Watenpaugh, K. D. (1999) The atomic-resolution structure of human caspase-8, a key activator of apoptosis. *Structure 7*, 1135−1143.
(46) Otwinowski, Z., and Minor, W. (1997) Processing of X-ray diffraction data collected in oscillation mode. *Meth. Enzymol. 276*, 307−326.
(47) McCoy, A. J., Grosse-Kunstleve, R. W., Adams, P. D., Winn, M. D., Storoni, L. C., and Read, R. J. (2007) Phaser crystallographic software. *J. Appl. Crystallogr. 40*, 658−674.
(48) The CCP4 suite: programs for protein crystallography (2004) *Acta Crystallogr., Sect. D: Biol. Crystallogr. 50*, 760−763.
(49) Chai, J., Wu, Q., Shiozaki, E., Srinivasula, S. M., Alnemri, E. S., and Shi, Y. (2001) Crystal structure of a procaspase-7 zymogen: mechanisms of activation and substrate binding. *Cell 107*, 399−407.
(50) Emsley, P., Lohkamp, B., Scott, W. G., and Cowtan, K. (2010) Features and development of Coot. *Acta Crystallogr., Sect. D: Biol. Crystallogr. 66*, 486−501.
(51) Adams, P. D., Afonine, P. V., Bunkóczi, G., Chen, V. B., Davis, I. W., Echols, N., Headd, J. J., Hung, L. -W., Kapral, G. J., Grosse-Kunstleve, R. W., McCoy, A. J., Moriarty, N. W., Oeffner, R., Read, R. J., Richardson, D. C., Richardson, J. S., Terwilliger, T. C., and Zwart, P. H. (2010) PHENIX: a comprehensive Python-based system for macromolecular structure solution. *Acta Crystallogr., Sect. D: Biol. Crystallogr. 66*, 213−221.
(52) Laskowski, R. A., MacArthur, M. W., Moss, D. S., and Thornton, J. M. (1993) PROCHECK: a program to check the stereochemical quality of protein structures. *J. Appl. Crystallogr. 26*, 283−291.
(53) Hooft, R. W., Vriend, G., Sander, C., and Abola, E. E. (1996) Errors in protein structures. *Nature 381*, 272.
(54) Chen, V. B., Arendall, W. B., Headd, J. J., Keedy, D. A., Immormino, R. M., Kapral, G. J., Murray, L. W., Richardson, J. S., and Richardson, D. C. (2010) MolProbity: all-atom structure validation for macromolecular crystallography. *Acta Crystallogr., Sect. D: Biol. Crystallogr. 66*, 12−21.
(55) Berman, H. M., Westbrook, J., Feng, Z., Gilliland, G., Bhat, T. N., Weissig, H., Shindyalov, I. N., and Bourne, P. E. (2000) The Protein Data Bank. *Nucleic Acids Res. 28*, 235−242.